October 2019, No 5

Hellenic Neutron Association Newsletter

Editorial

In the fifth issue of the HENA newsletter two research notes are presented by our colleagues Dr Christine Papadakis and Dr Antigoni Theodoratou. The first refers to the use of various neutron methods to tune the hydration state of thermoresponsive polymers under pressure, trying to understand molecular interactions and macroscopic behavior. In the second one, neutron reflectometry is used to study the adsorption of proteins on vegetable oil hybrid films in an effort to evaluate a new biomaterial that can be used in biomedicine as artificial material for implants and transdermal drug delivery systems. Enjoy reading them!

— Dr. Konstantina Mergia (NCSR Demokritos)

Research Note: What can pressure do for the understanding of thermoresponsive polymers? *

by Bart-Jan Niebuur‡ , Alfons Schulte †, and Prof. Christine M. Papadakis ‡

Thermoresponsive polymers in aqueous solution feature lower critical solution temperature behavior, i.e. they are water-soluble below a certain temperature, but water-insoluble above [1]. At the transition, the polymers collapse and form large aggregates. This behavior is due to the special interactions of the polymers with water, namely by hydrogen bonding via polar side groups and by hydration of hydrophobic moieties. In that respect, synthetic thermoresponsive polymers with simple molecular structures may serve as model systems for the folding and aggregation behavior of the-often substantially more complex-biological macromolecules. Moreover, thermoresponsive polymers find applications in switches, e.g. in microfluidic chips, or for smart transport and release purposes [2]. The time scales as well as the reversibility and reproducibility of the switching process depend largely on the molecular interactions, the change of chain conformation and the aggregation mechanism.

*The authors are indebted to M.-S. Appavou, W. Lohstroh, V. Pipich, (all Maier-Leibnitz Zentrum, Garching) and L. Chiappisi (Institut Laue-Langevin, Grenoble) for support with the experiments. The MLZ and ILL are thanked for beamtime allocation and excellent equipment. Funding by Deutsche Forschungsgemeinschaft, the TUM August-Wilhelm Scheer Guest Professor Program and the Faculty Graduate Center Physics of the TUM Physics Department are gratefully acknowledged.

†University of Central Florida, Department of Physics and College of Optics and Photonics, Orlando, FL, U.S.A.
‡Technical University of Munich, Physics Department, Soft Matter Physics Group, 85748 Garching, Germany

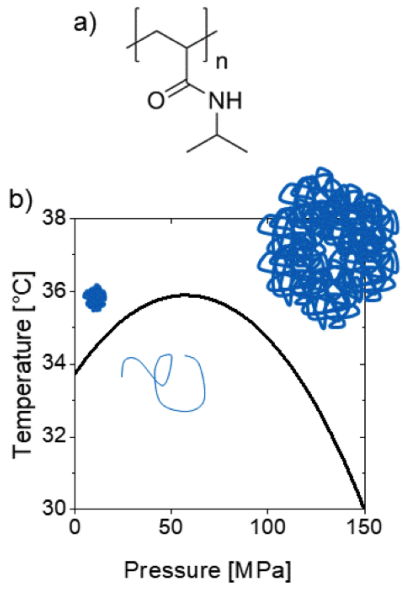

Figure 1. (a) Chemical structure of PNIPAM. (b) Phase diagram of a 3 wt% PNIPAM solution in D_2O in the temperature-pressure frame (black line). While the polymer is molecularly dissolved at low temperatures, and the solution is in the one-phase state, the polymer is collapsed and forms aggregates above. Data in (b) are from Ref. 7.

A prominent representative of thermoresponsive polymers is poly(N-isopropylacrylamide) (PNIPAM, Figure 1a) [3]. Its backbone is hydrophobic, whereas its side group features a hydrophobic isopropyl side group as well as a polar amide group. While the latter can form hydrogen bonds with water (and with adjacent side groups), hydrophobic hydration occurs around the hydrophobic moieties, i.e. the formation of structured water. The temperature-driven transition of this polymer in aqueous solution as well as its molecular origin have been amply studied, but conclusive understanding has not been achieved yet. For instance, it is unclear why the aggregates formed by PNIPAM above the transition temperature do not continue to grow until macroscopic phase separation is reached. Instead, rather compact aggregates of mesoscopic size are formed (Figure 1b), which are long-lived and frequently are called "mesoglobules". The pathway of aggregation after the collapse of the chains is key for the switching properties of thermoresponsive materials. Neutron methods, such as time-resolved small-angle neutron scattering (SANS), can give a wealth of structural information in a time-resolved manner; however, it is not straightforward to realize the fast temperature changes across the phase transition which are needed to investigate the full transition from the molecularly dissolved chains to the mesoglobules, since oftentimes neutron methods require relatively large sample volumes.

The interactions of PNIPAM with water are sensitive to the application of high pressure due to, among others, alterations of the structure of the hydration layer around apolar and polar groups [4]. Indeed, the transition temperature is pressure-dependent, leading to an elliptical coexistence line in the temperature-pressure frame (Figure 1b). This opens up for investigations of the aggregation behavior under different hydration conditions, namely by crossing the coexistence line in temperature scans at different pressures or by isothermally changing the pressure. Moreover, pressure can be changed rapidly (at sub-second time scales) without thermal effects. Thus, pressure jumps along with time-resolved structural measurements allow monitoring the collapse and aggregation behavior in real time.

In our work, we revisited the aggregation behavior of aqueous PNIPAM solutions, making use of these new possibilities. In addition to the commonly used laboratory methods, such as turbidimetry, light scattering and optical microscopy, we applied a number of neutron methods to obtain comprehensive information: Quasi-elastic neutron scattering (QENS) was used to investigate the dynamics of the hydration water of PNIPAM [5]. Very small angle neutron scattering (VSANS) allowed characterizing the aggregates in terms of their size and water content at different pressures [6]. Time-resolved SANS was used to follow the pathways of aggregate formation after pressure jumps from the one-phase to the two-phase state [7,8]. Here, we summarize a few of the results to showcase the opportunities offered by high pressure.

Water dynamics at low and at high pressure

QENS has been amply used to investigate the dynamics of water, both bulk water and hydration water of thermo-responsive polymers at atmospheric pressure [9,10]. We carried out temperature scans on a concentrated (25 wt%) PNIPAM solution in H_2O around the transition temperatures at atmospheric pressure and at 130 MPa to probe the change of the interaction of PNIPAM with water [5]. At this, the instrument TOFTOF at MLZ, Garching, was used along with a high pressure cell having rod-like cavities in a thermostated Al pressure cell [11]. A high polymer concentration was chosen to ensure that a large fraction of water is in contact with the chain. From the intermediate dynamic structure factors, we calculated the frequency-dependent dynamic susceptibility $\chi''(\nu)$ to distinguish the contribution of hydration water (at $\approx 10^1$ GHz) from the ones from bulk water at higher frequencies (Figure 2a,b).

The $\chi''(\nu)$ data show that, at atmospheric pressure, the contribution of hydration water decreases abruptly at the transition temperature (i.e. within 1 K, Figure 2a). In contrast, at 130 MPa, this contribution decreases smoothly over a range of more than 10 K (Figure 2b). This is quantified by model fitting, which reveals that the fraction of hydration water decreases abruptly at the transition temperature (i.e. within 1 K) at atmospheric pressure, but smoothly at 130 MPa (Figure 2b). In particular, at high pressure, the PNIPAM chains are more hydrated in a temperature range of several degrees Celcius above the transition temperature than at atmospheric pressure.

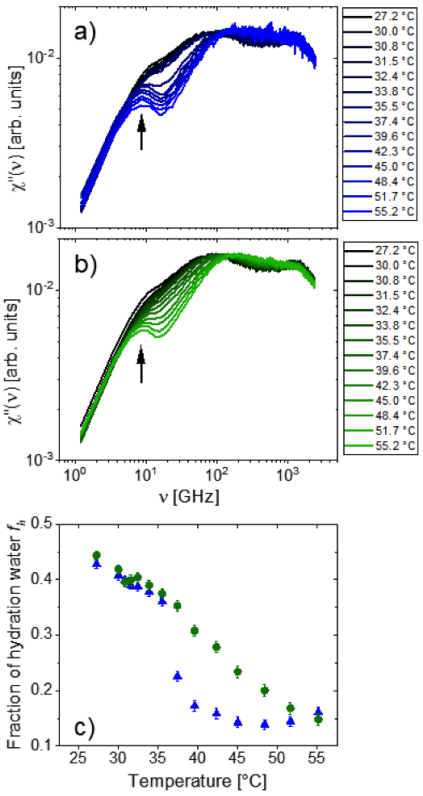

Figure 2. (QENS susceptibility spectra χ'' of a 25 wt% PNIPAM solution in H_2O as a function of frequency ν in dependence on temperature during heating scans. The spectra are taken at a momentum transfer $q = 1.65$ Å^{-1} at a pressure of 0.1 MPa (a) and 130 MPa (b) and the temperatures given in the graphs. The arrows in (a) and (b) mark the contribution of hydration water. The higher frequency processes are due to bulk water. (c) Relative fraction of hydration water f_h in dependence on temperature at atmospheric pressure (blue circles) and at 130 MPa (green circles). Data from Ref. 5.

Aggregates at low and high pressure

The tunability of the dehydration of PNIPAM at the transition temperature by pressure may be exploited to investigate the aggregation behavior under strong and weak dehydration conditions. We chose VSANS to determine the size of the mesoglobules in a 3 wt% PNIPAM solution in D_2O [6]. Instrument KWS-3, MLZ, offered the necessary q resolution. A temperature-controlled pressure cell was used, where the pressure was transmitted to the sample via a deformable O-ring [12].

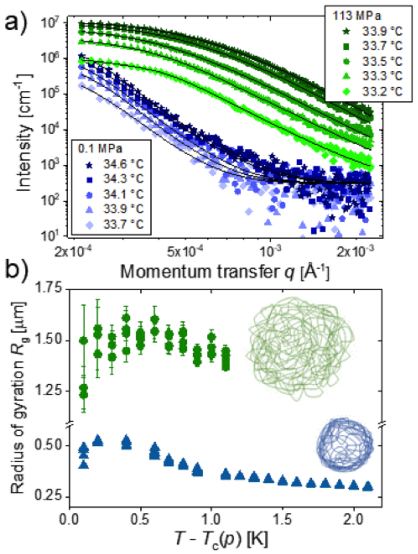

Figure 3. (a) Representative VSANS data of the 3 wt% PNIPAM solution in D_2O from temperature scans at atmospheric pressure (blue symbols) and at 113 MPa (green symbols), all above $T_c(p)$. $T_c(p)$ is the transition temperature at the given pressure p. The black lines are model fits. (b) Radius of gyration of the mesoglobules in dependence on reduced temperature at atmospheric pressure (blue symbols) and at 113 MPa (green symbols). All data from Ref. 6. The sketches indicate the aggregate structure and water content.

In heating scans through the transition temperature, a sudden increase of the scattering intensity was observed at the cloud point, which is due to scattering from mesoglobules (Figure 3a). Above the transition temperature, the decays at 113 MPa are shifted to lower q values compared to atmospheric pressure. Model fitting revealed that this shift is due to distinctly larger aggregate sizes at 113 MPa ($\approx$ 1.5 μm, Figure 3b) than at atmospheric pressure ($<$ 0.5 μm). Moreover, the inner structure of the aggregates differs significantly: At atmospheric pressure, the mesoglobules are surrounded by a dense shell, which is formed as water leaves the aggregates rapidly at an early stage. We suspect that this dense shell hinders further coalescence of the mesoglobules and may be at the origin of their longevity. Such a shell is not formed at high pressure, the aggregates contain a significant amount of water and are much larger.

Pathway of aggregate formation at low and at high pressure

The strong difference in dehydration at the transition temperature at low and high pressures may be expected to result in very different pathways of aggregation as well: At low pressures, dehydration is strong and shell formation hinders the mesoglobule growth, therefore, one may anticipate several growth stages. In contrast, at high pressure, aggregation seems thermodynamically less favorable, but less kinetic hindrances to the growth are imposed by viscoelastic effects. We show here the results from two pressure jumps from the one-phase to the two-phase state: One jump from the one-phase regime to low pressures (i.e. from 31 to 16 MPa) [7] and one to higher pressures (i.e. from 87 to 101 MPa) [8]. To rule out thermal effects, both jumps were carried out at the same temperature (35 °C). These jumps were realized by a high-pressure copper beryllium cell, where pressure is transmitted to the sample via a movable piston [13]. The pressure jump was accomplished within 0.1 s by means of a pneumatically driven valve. Again, a 3 wt% solution of PNIPAM in D_2O was used. Time-resolved SANS measurements were carried out at instrument D11, ILL, with a time resolution of 0.05 s.

The time-resolved SANS data from the two jumps are shown in Figure 4a and b. In both cases, the pre-release curves are characteristic of semidilute solutions undergoing concentration fluctuations. For the low pressure jump, this state is maintained at early times (Figure 4a), but soon an additional contribution appears at low momentum transfers, which reflects the formation and growth of mesoglobules from collapsed chains. At later stages, the increase becomes weaker. Fitting of structural models yields

the correlation length and the radius of gyration of the mesoglobules and thus information on the underlying mechanisms (Figure 4c). The increasing correlation length of the concentration fluctuations ξ indicates the formation of small clusters by a nucleation and growth mechanism. Then, mesoglobules are formed, and their radius of gyration R_g increases with time according to a power law $R_g(t) \propto t^{1/3}$, i.e. they grow by diffusion-limited coalescence [14]. The formation of the dense shell is observed as well (not shown). Eventually, the growth follows $R_g(t) \propto log(t)$, suggesting the appearance of an energy barrier of several k_BT that hinders further coalescence and makes the mesoglobules long-lived [15]. This energy barrier may be attributed to the dense shell which hinders the coalescence of two mesoglobules because of the low mobility of the polymers [16].

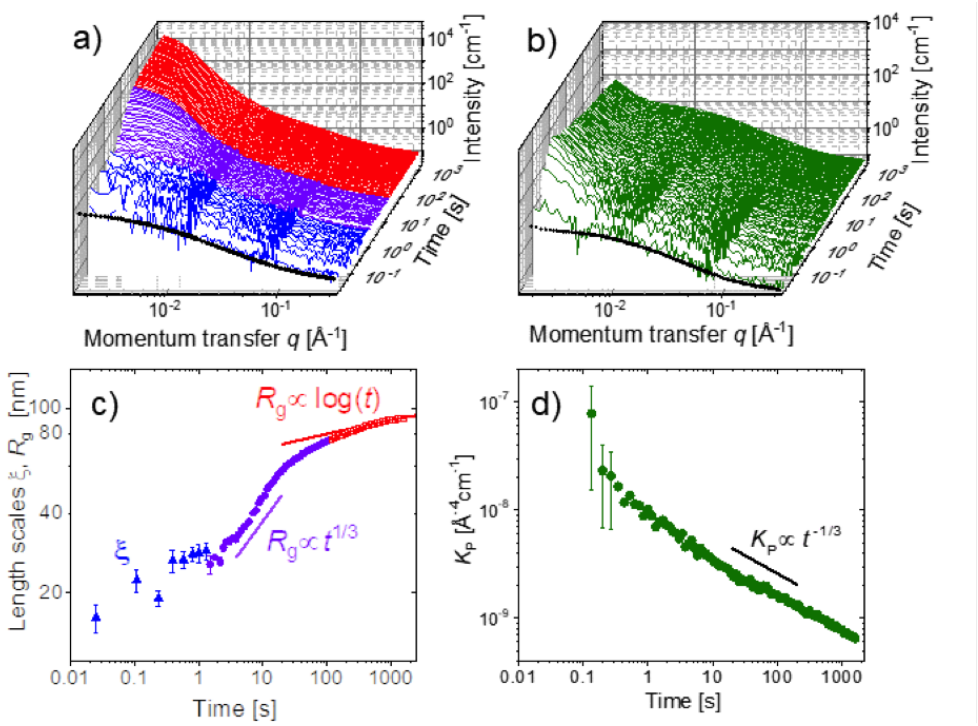

Figure 4. Time-resolved SANS data of the 3 wt% PNIPAM solution in D_2O after the jumps from 31 to 16 MPa (a) and from 87 to 101 MPa (b), both at 35.1 °C. Black symbols: pre-release measurements. (c) Time dependence of the correlation length and the radius of gyration of the mesoglobules from the data in (a). In (a) and (c), the 3 growth regimes are indicated by different colors. (d) Time dependence of the Porod constant of the aggregates in (b).

For the high-pressure jumps, the behavior is significantly different (Figure 4b). Directly after the jumps, an additional contribution at low q values appears, which shows that, immediately, loosely packed clusters consisting of several chains form. Its intensity increases rapidly and becomes a straight line in the double-logarithmic representation with a slope of approximately q^{-4}, which points to compact and very large aggregates, in consistency with our previous, static observations. During the remaining time, the intensity of the aggregate scattering decreases slightly; thus, the aggregates grow during the entire run. The scattering at high q values due to concentration fluctuations is still present, which is related to the high water content inside the aggregates. Model fitting of, among others, a Porod term describing the aggregate scattering reveals that the amplitude of this term, K_p, decreases during the entire run following a $t^{-1/3}$ behavior (Figure 4d). K_p is proportional to the specific surface of the aggregates. Assuming that these are spherical, K_p is inversely proportional to the radius of the aggregates R. We conclude that $R \propto t^{1/3}$, which is consistent with the growth by diffusion-limited coalescence [14]. In contrast to the low-pressure regime, this growth continues during the entire measuring time (≈ 2000 s). The coalescence of the aggregates is not hindered by any energy barrier, and eventually, macroscopic phase separation may be expected.

Summary

Neutron methods in combination with high pressure allow to tune the hydration state of the thermoresponsive polymer PNIPAM in aqueous solution and to further our understanding of the switching behavior. Combining QENS, VSANS and time-resolved SANS, we have shown that the fraction of hydration water in the

two-phase state indeed depends on pressure, which has a strong effect on the size, inner structure and water content of the mesoglobules as well as on the pathway of aggregate formation. Pressure jumps enabled accessing the structural evolution at very early times which cannot easily be reached by temperature jumps. Our results are complementary to the ones gained from other spectroscopic methods, such as FT-IR and Raman spectroscopy, light scattering and optical microscopy. The presented strategies may be applied to more complex systems, such as other thermoresponsive polymers, possibly of more complex architecture, and to biopolymers and proteins, bridging the gap between molecular interactions and macroscopic behavior.

(1) V. Aseyev, H. Tenhu and F. M. Winnik, "Non-Ionic Thermoresponsive Polymers in Water", Adv. Polym. Sci. 242, 29-89 (2011).

(2) M. Wei, Y. Gao, X. Li and M. J. Serpe, "Stimuli-Responsive Polymers and their Applications", Polym. Chem. 8, 127 (2017).

(3) A. Halperin, M Kröger and F. M. Winnik, "Poly(N-isopropylacrylamide) Phase Diagrams: Fifty Years of Research", Angew. Chem. Int. Ed. 54, 15342 (2015).

(4) V. M. Dalardat and C. B. Post, "Decomposition of Protein Experimental Compressibility into Intrinsic and Hydration Shell Contributions, Biophys. J. 91, 4544 (2006).

(5) B.-J. Niebuur, W. Lohstroh, M.-S. Appavou, A. Schulte and C. M. Papadakis, "Water Dynamics in a Concentrated Poly(N-isopropylacrylamide) Solution at Variable Pressure", Macromolecules 52, 1942 (2019).

(6) B. J. Niebuur, K.-L. Claude, S. Pinzek, C. Cariker, K. N. Raftopoulos, V. Pipich, M.-S. Appavou, A. Schulte and C. M. Papadakis, "Pressure-dependence of Poly(N-isopropylacrylamide) Mesoglobule Formation in Aqueous Solution", ACS Macro Lett. 6, 1180 (2017).

(7) B.-J. Niebuur, L. Chiappisi, X. Zhang, F. Jung, A. Schulte and C. M. Papadakis. "Formation and Growth of Mesoglobules in Aqueous Poly(N-isopropylacrylamide) Solutions Revealed with Kinetic Small-Angle Neutron Scattering and Fast Pressure Jumps", ACS Macro Lett. 7, 1155 (2018).

(8) B.-J. Niebuur, L. Chiappisi, F. Jung, X. Zhang, A. Schulte and C. M. Papadakis, "Kinetics of Mesoglobule Formation and Growth in Aqueous Poly(N-isopropylacrylamide) Solutions: Pressure Jumps at Low and at High Pressure", Macromolecules 52, 6416 (2019).

(9) M. Philipp, K. Kyriakos, L. Silvi, W. Lohstroh, W. Petry, J. K. Krüger, C. M. Papadakis and P. Müller-Buschbaum, "From Molecular Dehydration to Excess Volumes of Phase-Separating PNIPAM Solutions", J. Phys. Chem. B 118, 4253 (2014).

(10) N. Osaka, M. Shibayama, T. Kikuchi and O. Yamamuro, "Quasi-Elastic Neutron Scattering Study on Water and Polymer Dynamics in Thermo/Pressure Sensitive Polymer Solutions", J. Phys. Chem. B 113, 12870 (2009).

(11) M.-S. Appavou, S. Busch, W. Doster, A. Gaspar and T. Unruh, "The Influence of 2 kbar Pressure on the Global and Internal Dynamics of Human Hemoglobin Observed by Quasielastic Neutron Scattering" Eur. Biophys. J. 40, 705 (2011).

(12) J. Kohlbrecher, A. Bollhalder, R. Vavrin and G. Meier, "A High Pressure Cell for Small Angle Neutron Scattering up to 500 MPa in Combination with Light Scattering to Investigate Liquid Samples", Rev. Sci. Instrum. 78, 125101 (2007).

(13) https://www.ill.eu/users/support-labs-infrastructure...

(14) R. Stepanyan, J.G.J.L. Lebouille, J.J.M. Slot, R. Tuinier and M.A. Cohen-Stuart, "Controlled Nanoparticle Formation by Diffusion Limited Coalescence", Phys. Rev. Lett. 109, 138301 (2012).

(15) K. Kyriakos, M. Philipp, J. Adelsberger, S. Jaksch, A.V. Berezkin, D.M. Lugo, W. Richtering, I. Grillo, A. Miasnikova, A. Laschewsky, P. Müller-Buschbaum and C.M. Papadakis, "Cononsolvency of water/methanol mixtures for PNIPAM and PS-*b*-PNIPAM: Pathway of aggregate formation investigated using time-resolved SANS", Macromolecules 47, 6867 (2014).

(16) H. Tanaka, "Viscoelastic Phase Separation", J. Phys.: Condens. Matter 12, R207 (2000).

Research Note: Neutron-Reflectometry used as tool for the detection of adsorbed proteins on vegetable oil hybrid films [§]

by Dr. Antigoni Theodoratou [¶]

Neutron reflectometry (NR) is a powerful tool for measuring the structure of thin films, providing valuable information in applications including protein adsorption and aggregation and it is particularly applied to studies related to wet interfaces, where one of the surfaces is a liquid. Using neutron reflection to study the interfacial layer between two phases, a neutron beam passes through one of the phases to reach the interface. Due to the transparency of many liquid films, neutron reflectometry is very effective for the detection of buried interfaces and immersed layers. In the literature many proteins have been studied at liquid-liquid and solid-liquid interfaces using NR [1-3] mainly due to understanding of the relationship between protein molecular structures and their emulsifying properties. However, our knowledge of protein conformations at fluid interfaces is still limited and the denaturation of proteins has not been understood. In our recent work [4], we have created nanofilms of thickness of about two nanometers at the air-water interface using functionalized castor oil (ICO) with crosslinkable silylated groups. When ICO is spread at the air-water interface, a sol-gel reaction occurs via a hydrolysis and condensation step leading to the formation of a hybrid film. The importance of this material is that it represents an excellent candidate for replacing conventional polymeric materials in biomedical applications. The challenge was to optimize bio-

[§]The author would like to thank Julian Oberdisse , Lay-Theng Lee and Anne Aubert- Pouëssel for fruitful discussions and the collaboration and to acknowledge the French Neutron Federation F2N and the French national neutron scattering laboratory, Laboratoire Léon Brillouin (CEA-Saclay) for beam time.

[¶]Université de Montpellier, Montpellier, France

compatibility which is highly related to protein adsorption. NR has been used to study the adsorption of two model proteins, bovine serum albumin and lysozyme, at the silylated oil (ICO)-water interface in the absence and presence of salt at physiologic ionic strength and pH and at different protein concentrations. To compare our results in the presence of the film with a reference system, we have also characterized the adsorption of the aforementioned proteins at the air-water interface.

Experimental Part and Fitting Procedure

Specular neutron reflectivity experiments were performed on the time-of-flight neutron reflectometer Hermes at the ORPHEE reactor in Laboratoire Léon Brillouin (LLB) at CEA-Saclay using a polychromatic beam with wavelength $\lambda \approx 2.5$ to 25 Å. The horizontal beam was bent using a supermirror onto the liquid surface with a grazing incident angle of $\theta = 1.6^o$ and an angular resolution of $\delta\theta/\theta = 0.07$ that corresponds to a momentum transfer range of $q = 4\pi \sin\theta/\lambda$ (0.014 to 0.14 Å^{-1}). Here, all measurements were carried out at room temperature at 22 - 23 °C. The reflectivity curves were fitted using a model of n-layers with constant scattering length density, ρ. The scattering length density is defined as $\rho = N_A \sum(\delta_j/A_j)b_j)$ where N_A is the Avogadro's number, and δ_j, A_j and b_j are the mass density, atomic weight and coherent scattering length of atom j respectively. In order to subtract the background noise, we used a constant value (2x10^{-6}), that corresponds to the incoherent signal of deuterium at high Q. For the n-layer model, the scattering length density profile is given by:

$$\rho(z) = \sum_{n=0}^{N} \left(\frac{\rho_i - \rho i + 1}{2}\right)\left(1 - erf\frac{z - z_i}{\sigma_i}\right) \quad (1)$$

The fitted parameters are the scattering length density ρ_i, the thickness $d_i = z_i - z_{(i+1)}$ of each layer i and the interfacial roughness between layer i and $i+1$ described by an error function σ_i. To obtain the best-fit parameters, the experimental and calculated curves by iteration and minimization of the χ^2 parameter were compared. After the estimation of the scattering length density profile, $\rho(z)$, the protein volume fraction ϕ_p can be extracted using the following relation:

$$\rho = \phi_p\rho_p + (1 - \phi_p)\rho_s \quad (2)$$

where ρ_p and ρ_s are the scattering length densities of the protein and the solvent respectively. From the protein volume fraction profile, the total adsorbed density, Γ, in mg ·m^{-2}, can be calculated from:

$$\Gamma = \delta_p \times \phi_p \times d \quad (3)$$

where δ_p is the bulk density of the protein, d is the thickness of the layer, and ϕ_p the protein volume fraction found from Eq. (2).

Results

A didactical comparison of reflectometry curves measured for different interfaces is shown in Figure 1A. The first spectra show the reflectivity for the solvent at the air-D_2O interface, the second spectra show the adsorbed lysozyme at the air-D_2O interface, and the third spectra show the adsorbed lysozyme at the ICO-D_2O interface. All spectra have been plotted as a function of $R \cdot q^4$ versus q in order to give emphasis to the high-q regime. The solid lines are the best-fits with their corresponding scattering length density profiles (SLD) shown in Figure 1B. It's worth mentioning that the peak located at 0.02 Å^{-1} is the critical total reflection edge q_c from which the scattering length density of the subphase is deduced. Also, with respect to the D_2O subphase alone, the presence of adsorbed proteins and of oil decreases the neutron reflectivity due to the lower scattering length densities of the proteins and the oil compared to the scattering length density of the deuterated water. Consequently, the higher the protein adsorption, the lower the reflectivity signal. A schematic representation of the protein concentration profile is shown in Figure 1C.

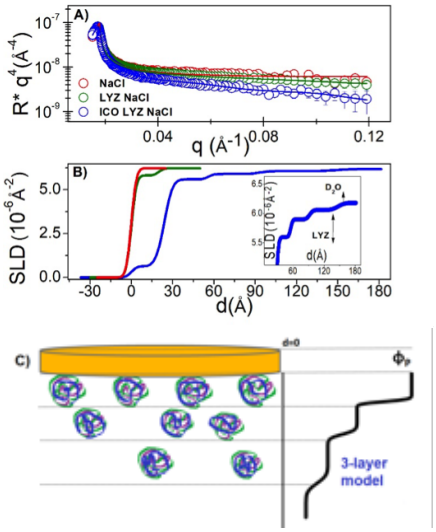

Figure 1. Neutron reflectivity curves (A) for the adsorption of lysozyme at the air-D_2O (green) and ICO-D_2O (blue) interface (155 mM NaCl); the curve for the solvent is also shown (red). The solid lines are the best fits with their corresponding scattering length density profiles shown in (B) with a zoom for the ICO-D_2O interface shown in the inset. In (C) a cartoon of the protein layer model with its volume fraction profile $\phi_p(d)$ is represented.

Proteins at the oil-water interface. In Figure 2A the reflectivity curves for the adsorption of BSA and lysozyme at the ICO-water interface are shown. Here, the fitted scattering length density for the oil layer does not vary significantly, its average fitted SLD value is 0.61 × 10^{-6}Å^{-2} which is very close the calculated value for pure ICO that is 0.57 × 10^{-6}Å^{-2}. Due to spreading error the thickness of the oil layer was found to vary from 21 to 25 Å. In Figure 2B the corresponding protein volume fraction profiles extracted from the fitted layers are shown. As depicted in the inset schematic representation in Figure 2B, the protein profile begins at the oil-solvent interface ($d = 0$). For both proteins in D_2O, a 2-layer model is necessary to give a good fit while in the presence of 155 mM NaCl a 3-layer model is required. From the concentration profiles, the effect of salt can be seen clearly from the total thickness of the adsorbed protein layer.

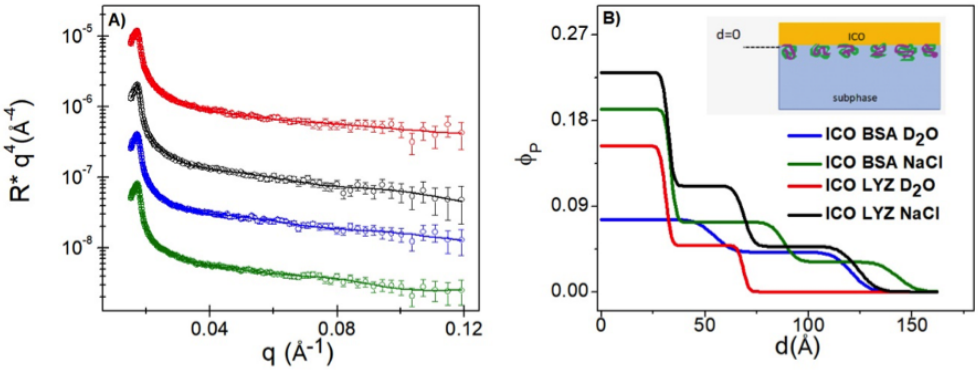

Figure 2: Adsorption of proteins at the oil (ICO) -water interface showing the effect of each protein and the effect of salt. In (A) the neutron reflectivity plots as a function of $R \cdot q^4$ versus q are shown. The curves have been separated vertically for clearer viewing. The solid lines are best-fits and their corresponding volume fraction profiles are shown in (B).

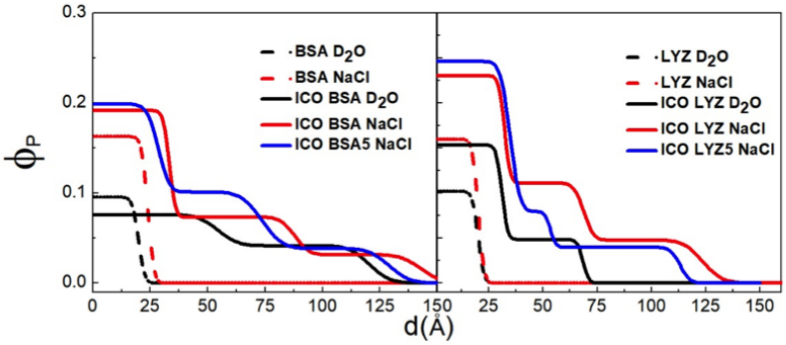

Figure 3: Summary of adsorption density profiles at the air-water (dashed lines) and (ICO) oil-water (solid lines) interfaces. In the left panel the adsorption of BSA is shown and in right panel the adsorption of lysozyme. In D_2O at $C_p = 1$ mg $\cdot$ mL^{-1} (black); in D_2O (155 mM NaCl) at $C_p = 1$ mg $\cdot$ mL^{-1} (red) and at $C_p = 5$ mg $\cdot$ mL^{-1} (blue).

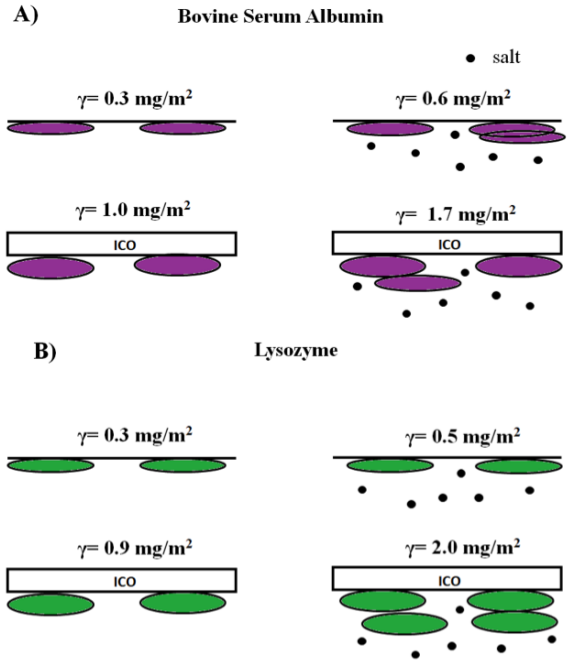

Figure 4: Schematic representation of protein adsorption of BSA (A) and lysozyme (B) at the air-water (top) and ICO-water (bottom) interface, in the presence and absence of salt (represented by dots). The figure is intended to show an approximate representation of the adsorbed molecule's orientation; with each layer not to necessarily correspond to the exact molecular position within the adsorbed layer.

In Figure 3, we present the concentration profiles for each protein in order to compare the adsorption at the air-D_2O and oil-D_2O interface. The difference is significant between the adsorption behavior at the air-water and ICO-water interfaces; the adsorption at the air-D_2O interface can be described by a 1-layer model, due to the low adsorption, while at the oil-D_2O interface a 2-layer and 3-layer models have been used to characterize the protein layer which extends to a total thickness that indicates multilayering. Consequently, at the ICO-D_2O interface, both the total adsorbed layer thickness and the packing density were increased. Regarding the salt effect, the increased adsorption (see γ in Figure 4) due to salt addition is also evident at both interfaces and for both proteins. In Figure 4 a schematic of their approximate adsorbed orientation is shown.

Conclusions

Neutron reflectivity is a very sensitive technique compared to other techniques for the structural characterization of macromolecules at the air-water and oil-water interfaces as the good neutron reflection contrast between the solvent and the film can allow accurate measurements. In this work, the protein adsorption behavior has been characterized for the evaluation of a new biomaterial, that can be used in biomedicine as artificial material for implants and transdermal drug delivery systems. Neutron reflectivity has been employed as a powerful tool to examine the adsorption of two model proteins, bovine serum albumin and lysozyme at the ICO-water interface. The effects of salt with an ionic strength close to the physiological concentration and of protein bulk concentration have been also investigated. Our key result consists in the identification of the most favorable and unfavorable conditions for which protein adsorption on the ICO nanofilms occurs. Notably, the volume fraction profiles suggest that in the main layer (oil-side), the proteins adsorb with their long axis parallel to the surface and the presence of salt in the subphase increases their packing density in this layer, leading to multilayer adsorption.

(1) J. Penfold, R.K. Thomas, E. Simister, E. Lee, A. Rennie, The structure of mixed surfactant monolayers at the air-liquid interface, as studied by specular neutron reflection, Journal of Physics-Condensed Matter 2 (1990) 411-416.
(2) J.R. Lu, T.J. Su, J. Penfold, Adsorption of serum albumins at the air/water interface, Langmuir 15(20) (1999) 6975-6983.
(3) J.R. Lu, T.J. Su, R.K. Thomas, Structural conformation of bovine serum albumin layers at the air-water interface studied by neutron reflection, Journal of Colloid and Interface Science 213(2) (1999) 426-437.
(4) A. Theodoratou, L.T. Lee, J. Oberdisse, A. Aubert-Pouessel, Equilibrium Protein Adsorption on Nanometric Vegetable Oil Hybrid Film/Water Interface Using Neutron Reflectometry, Langmuir 35(20) (2019) 6620-6629.

Schools

ISIS Practical Neutron Training Course

Applications are now invited for the annual ISIS Practical Neutron Training Course, which will take place 10 -19 March 2020. It is aimed at PhD and post-doctoral researchers who have little or no experience of practical neutron scattering, but whose future research program aims to make use of neutron scattering techniques at ISIS. The course is free to attend and accommodation is provided. Registration is via the course website and is open until November 20th. The course is always highly oversubscribed and so there will be no extensions to the deadline. The website provides details of the selection criteria used when assessing applications.

HERCULES 2020 - European School

2020 session: 2 March-3 April, 2019

DEADLINE FOR APPLICATION: 31 October, 2019

HERCULES is a European course for PhD students and young researchers using Neutrons and Synchrotron Radiation for applications in Biology, Chemistry, Physics, Hard Soft Condensed Matter.

The 5-week school includes lectures (60%), hands-on practicals and tutorials. Exceptionally in 2020, because of the long ESRF shutdown, participants will spend two weeks in two different partner institutions in Europe among:

- ALBA synchrotron in Barcelona, Spain
- KIT light source in Karlsruhe, Germany
- DESY and European XFEL in Hambourg, Germany
- Elettra and FERMI in Trieste, Italy
- Soleil and LLB in Paris-Saclay, France
- PSI in Villigen, Switzerland

This comes in addition to tutorials or practicals which will take place in Grenoble at ILL, ESRF and Grenoble Laboratories (CEA, CNRS, EMBL, IBS).

The school includes a common part and two parallel sessions:

- Biomolecular, soft condensed matter structure dynamics
- Physics and chemistry of condensed matter

Why join Hercules ?

- to learn new techniques using neutron and synchrotron radiation

- to expand your theoretical and practical knowledge, not only for your present research but for your scientific career
- to experiment these techniques on world-class instruments beamlines
- to build a network of relations with fellow young researchers and experienced teachers from all around the World

Bursaries/reduced costs

- A limited number of bursaries will be available to reduce registration fees

Useful links

European Neutron Scattering Association

The European Neutron Scattering Association (ENSA) is an affiliation of national neutron scattering societies and committees, which directly represent users. The overriding purposes of ENSA are to provide a platform for discussion and a focus for action in neutron scattering and related topics in Europe.

SINE2020 Webpage

SINE2020 is a consortium of 18 partner institutions that is funded by the European Union through the H2020 programme. The website contains neutron community news and updates, and also interesting educational material.

Contact with the editorial board

The provisional editorial board welcomes articles and ideas about the contents of the HENA newsletter from fellow scientists in Greece and abroad. For this purpose please contact:

- Dr. Konstantina Mergia, NCSR Demokritos, Athens kmergia[at]ipta.demokritos.gr
- Asst. Prof. Dimitrios Anastassopoulos, Univ. of. Patras, anastdim[at]physics.upatras.gr
- Dr. Alexandros Koutsioumpas, Maier-Leibnitz Zentrum, Munich, a.koutsioumpas[at]fz-juelich.de